Pulse-width and focal-volume dependence of laser-induced breakdown

E. W. Van Stryland, M. J. Soileau,* Arthur L. Smirl, and William E. Williams
Physics Department, North Texas State University, Denton, Texas 76203
(Received 2 June 1980)

The laser-induced breakdown fields at 1.06 μm of fused SiO_2, single-crystal NaCl, and air were measured as a function of focal volume and laser pulse width while keeping all other parameters, including the specimen, constant. The laser pulse width was varied from 40 psec to 31 nsec, and the focal volume was varied by over two orders of magnitude. The dependence of the breakdown field for NaCl and SiO_2 on the laser pulse width t_p and the focal volume V was empirically determined to be $E_B = AV^{-1}t_p^{-1/4} + C$ and the dependence for air to be $E_B = (AV^{-1} + C)t_p^{-1/4}$, where A and C are material-dependent constants. Current theories of laser-induced breakdown are carefully compared with these present measurements and are found to be inconsistent.

I. INTRODUCTION

The laser-induced breakdown thresholds at 1.06 μm for fused SiO_2, single-crystal NaCl, and air were determined as a function of laser focal-spot size, for pulse widths ranging from 40 psec to 31 nsec. These experiments represent the first damage data, over a range of three orders of magnitude in pulse width, that clearly separate the temporal and spot size dependences of damage thresholds by keeping all parameters, including the specimen, constant. Recent work has shown that in many cases laser-induced breakdown thresholds vary greatly among specimens of a given material.[1-3] Thus, pulse-width and focal-spot size-dependence data are difficult to interpret, unless the same specimen is studied at all pulse widths and all focal-spot sizes. The present measurements demonstrate that the dependence on focal volume observed previously for nsec optical pulse widths also applies to the psec regime.[1] It is observed, over the range of pulse widths, t_p, and focal-spot sizes used in these experiments, that the electric field, E_B, necessary to induce breakdown for NaCl and SiO_2 varies as

$$E_B = A/(t_p^{1/4}V) + C \ , \tag{1}$$

and the breakdown field for air varies as

$$E_B = (A/V + C)/t_p^{1/4} \ , \tag{2}$$

where A and C are material-dependent constants, and V is the focal volume.[4] The depth of focus for a Gaussian beam focused by an aberration-free lens is proportional to ω_0^2/λ, where ω_0 is the $1/e^2$ radius of the intensity and λ is the laser wavelength. The focal volume is proportional to the depth of focus times the focal area; that is

$$V \propto \omega_0^4/\lambda \ . \tag{3}$$

The observed dependences of Eqs. (1) and (2) may explain many of the apparent discrepancies of pulse width and spot size dependences found in the literature. For example, for large focal volumes the temporal dependence of Eq. (1) is masked by the constant term, whereas for small focal volumes, where the first term dominates, the breakdown field would appear to scale as $t_p^{-1/4}$. Identical empirical fits for NaCl and SiO_2 imply that damage mechanism are similar in bulk samples of these two materials. For air, the pulse width dependence is quite different. The observed dependences on focal volume and pulse width, as well as the difference between the solid samples and air, are not explained by current theories of laser-induced breakdown. However, while the quantitative behavior cannot be explained, qualitatively the empirical fits presented above are consistent with the recently proposed multiphoton-initiated avalanche breakdown model presented in Refs. 1 and 2 and described in Sec. IV.

II. EXPERIMENT

The laser source for the psec studies was a passively mode-locked, microprocessor-controlled[5] Nd:YAG laser system operating at 1.06 μm. A single pulse of measured Gaussian spatial and temporal intensity distribution was switched from the mode-locked train

and amplified. The temporal pulse width was variable between 30 and 200 psec [full width at half maximum (FWHM)] by selecting various etalons as the output coupler. The width of each pulse was monitored by measuring the ratio, R, of the square of the energy in the fundamental (1.06 μm) to the energy in the second harmonic, produced in a $LiIO_3$ crystal. This ratio is directly proportional to the laser pulse width as long as the spatial profile remains unchanged.[6] The ratio was calibrated by measuring the pulse width using type-I second-harmonic autocorrelation scans. The observed three-to-one signal-to-background ratios indicated clean mode locking.[7] To ensure that the ratio, R, is proportional to the pulse width and provides a valid pulse width monitor, scans were performed for all three output coupler etalons.

The laser half-angle beam divergence was 0.38 mrad. The beam divergence and the position of the beam waist were determined by pinhole scans of the spatial profile at six positions along the propagation direction. Two lenses of focal lengths 5.0 and 8.0 cm were used at various distances from the beam waist to produce the focal-spot radii for these experiments. The lowest f-number condition used in these experiments was $f/7.4$. Spherical aberrations were determined to be negligible for this worst-case situation using the procedure suggested by Ireland *et al.*[8] Computation of spherical aberrations caused by a singlet lens indicated that errors in the field were less than 4% for the worst case. The lenses used however were doublets corrected for spherical aberration. Aberrations caused by focusing through the planar surfaces of the samples was calculated to cause an error in the field of less than 0.1% for the worst case. Diffraction limited performance of the 5.0-cm focal-length lens was verified by knife edge scans of the 6.1-μm radius spot.[1] The calculated 5.0-μm radius spot was subsequently scanned and verified to be diffraction limited to within the experimental uncertainty of ± 0.4 μm. The energy on target was varied by changing the angle between a calibrated pair of Glan polarizers that were arranged to keep the direction of polarization at the sample surface constant. The output energy of the laser and the energy transmitted through the sample were continuously monitored by sensitive photodiode peak-and-hold detectors. These detectors were determined to be linear over their range of use and were absolutely calibrated with respect to a pyroelectric energy monitor. The pyroelectric detector was in turn checked with a thermopile calorimeter.

The nsec data were taken on the *same* bulk samples using a Q-switched Nd:glass laser operated in the TEM_{00} mode.[1] The same focusing lenses were used, and the same procedures for determining the beam divergence (0.7 mrad) and beam waist were employed as for the psec measurements. Again, a calibrated pair of Glan polarizers were used to vary the energy on target. The laser output was monitored directly by a pyroelectric detector which was calibrated with the same calorimeter used for the psec experiments. The nsec pulse widths were determined directly from oscilloscope traces taken with a fast photodiode (rise time $\leq$500 psec).

The breakdown threshold at a given pulse width was taken to be that intensity which produced damage 50% of the time. Each site was irradiated only once. Damage was defined as the appearance of a visible flash or as the observation of scattered light from a coaxial HeNe laser as viewed through a 20×, long-working-distance microscope in accord with the methods used by previous investigators. The microscope was also used to verify that damage had occurred at the beam focus and was not due to inclusions. For psec damage to NaCl, there was a small range of incident energies where damage had occurred as determined from the scattered HeNe beam, but no flash was observed.

In addition to the 1-on-1 experiments, where each site was irradiated only once, an n-on-1 experiment was performed at the largest spot size (19.3 μm) for the solid samples. This was done by irradiating the same spot with one or more pulses of insufficient intensity to damage prior to irradiating with a damaging pulse. No measurable change in threshold was observed.

III. RESULTS

The results of these damage experiments are displayed in Fig. 1. All values quoted for electric

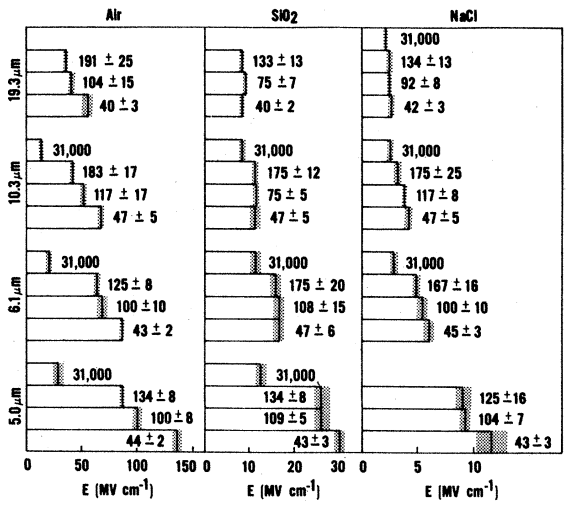

FIG. 1. Experimentally determined breakdown electric field, E_B, (rms), for air, SiO_2, and NaCl are tabulated for focused spot sizes ($1/e^2$ radius in intensity) of 5.0, 6.1, 10.3, and 19.3 μm and various optical pulse widths (FWHM) in psec, as indicated within or adjacent to the bars.

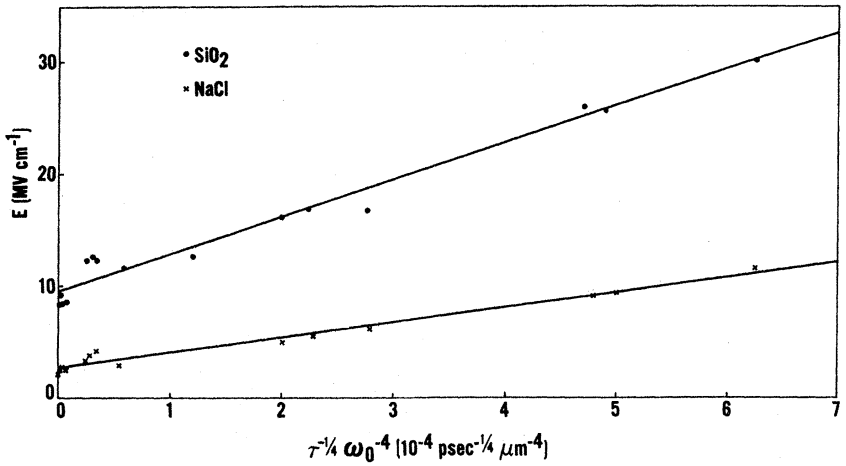

FIG. 2. rms breakdown electric field data for Harshaw single-crystal laser-grade NaCl and for General Electric high-purity water-free fused quartz is plotted as a function of $t_p^{-1/4}\omega_0^{-4}$ where t_p is the laser pulse width (FWHM) in psec and ω_0 is the focal-spot radius at the $1/e^2$ point in intensity in μm. The solid lines are least-squares fits of the data to straight lines.

field are rms fields corresponding to the peak on axis intensity. The error bars are relative errors determined by how well the threshold for damage is defined and the reproducibility of the data. The absolute errors include relative errors as well as errors in the measurement of the energy, focal-spot radius, and pulse width. These errors are estimated to be 20% for the breakdown electric fields.

The breakdown fields for NaCl and SiO_2 are plotted as a function of $t_p^{-1/4}V^{-1}$ in Fig. 2. Figure 3 is a plot of the product $t_p^{1/4}E_B$ as a function of V^{-1} for air.

Table I gives least-squares fits to straight lines for the data displayed in Figs. 2 and 3. From these fits it is seen that the breakdown field for air varies as $t_p^{-1/4}$ independent of the focal volume, whereas the breakdown fields in the solid materials appears nearly independent of pulse width for large focal volumes.

In addition we include previously unpublished data taken from the work of Ref. 1 in Table II. There the damage thresholds of a total of 13 different NaCl samples are given for three different focal-spot radii. All the data presented in Table II used 31-nsec

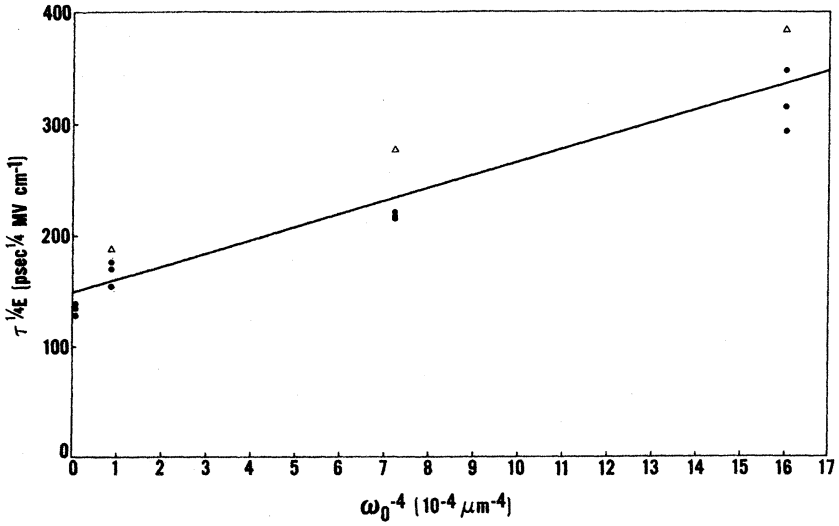

FIG. 3. Product $E_B t_p^{1/4}$ for air is plotted as a function of ω_0^{-4}. The rms breakdown field is E_B in MV/cm. t_p is the laser pulse width (FWHM) in psec and ω_0 is the focal-spot size ($1/e^2$ radius in intensity) in μm. The solid curve is a least-squares fit of the data to a straight line. The open triangles correspond to the 31-nsec data. The systematic deviation of the 31-nsec data from the fit is eliminated if the t_p dependence is changed to $t_p^{0.23}$ rather than $t_p^{0.25}$.

TABLE I. Empirical fits for the rms breakdown electric field (MV/cm) for the three materials studied, where t_p is the laser pulse width in psec (FWHM) and ω_0 in μm is the focused beam radius at the $1/e^2$ point in intensity. The NaCl is Harshaw (Harshaw Chemical Co., 6801 Cochron Road, Salon, Ohio 44139) single-crystal laser grade. The SiO_2 is high-purity, water-free fused quartz obtained from General Electric (General Electric No. 125, high-purity, water-free fused SiO_2 acquired from Mark Optics, 1510 East Street, Gertrude Road, Santa Anna, Calif. 92705).

NaCl	$E_B = \frac{1.36\,10^4}{t_p^{1/4}\omega_0^4} + 2.69$
SiO_2	$E_B = \frac{3.30\,10^4}{t_p^{1/4}\omega_0^4} + 9.52$
Air	$E_B = \left(\frac{1.16\,10^5}{\omega_0^4} + 150\right)\frac{1}{t_p^{1/4}}$

(FWHM) pulses. Table III gives the least-squares fits of the data of Table II to Eq. (1). Good fits are obtained for all the samples tested.

In the nsec experiments, the transmitted pulse was sharply terminated near the peak by the laser-induced plasma, resulting in approximately 50% transmission. This is in contrast to the greater than 80% transmission observed for the psec pulses. In addition, a slight trend toward higher transmission at the shortest pulse widths was evident. Thus, either breakdown takes place near the end of the pulse, or the breakdown process takes place on a time scale of the order of the pulse width. A third possibility that appears inconsistent with our nsec measurements but consistent with the psec data is that the plasma blocks transmission for a period short compared to the psec pulses used. Anthes and Bass,[9] using psec pulses, have made streak camera recordings of the transmitted damaging pulses in fused quartz at 0.53 μm. They found that the avalanche blocked transmission near the peak of the pulse in a time shorter than the 6-psec streak camera resolution. However, they also noted that the transmission recovered on a psec time scale. In point of fact, they observed approximately 80% transmission similar to the psec studies reported here.

TABLE II. The rms breakdown electric field (MV/cm) for NaCl samples using 31-nsec (FWHM) 1.06-μm pulses of focal spot radius ω_0 ($1/e^2$ radius in intensity) as indicated. Sample 6 is the sample used for the psec data.

Sample	ω_0 (μm) 6.1	10.3	19.3
1	4.17	3.18	2.92
2	4.24	3.45	3.13
3	4.12	3.39	2.68
4	3.05	1.89	1.97
5	1.44	1.18	0.99
6	3.10	2.57	2.14
7	5.46	4.03	3.67
8	6.67	3.85	3.90
9	4.86	4.13	3.03
10	4.81	3.93	3.89
11	5.36	3.58	3.54
12	4.64	4.13	3.78
13	5.20	3.81	3.59

TABLE III. Empirical fits for the rms breakdown electric field (MV/cm) to Eq. (1) of the text for the samples of NaCl of Table II. The laser pulse width is t_p which is in all cases 31 000 psec (FWHM), and ω_0 in μm is the focused beam radius at the $1/e^2$ point in intensity. R^2 is the coefficient of determination which is a measure of how closely the equations fit the experimental data. The closer R^2 is to one, the better the fit.

Sample	A (10^4)	C	R^2
1	2.31	2.96	0.996
2	1.98	3.21	0.985
3	2.32	2.93	0.918
4	2.27	1.84	0.988
5	0.751	1.05	0.948
6	1.58	2.28	0.938
7	3.31	3.72	0.997
8	5.62	3.68	0.992
9	2.79	3.45	0.862
10	1.82	3.85	0.998
11	3.63	3.43	0.996
12	1.45	3.89	0.953
13	3.06	3.59	0.999

IV. DISCUSSION

The problem of laser-induced breakdown of highly transparent materials has been studied by many workers[10] and has been the subject of at least three review papers.[11–13] Laser-induced breakdown in NaCl was first studied in 1966 by Olness[14] and in 1968 by Yasojima *et al.*[15] and has been extensively studied since that time. However, direct comparison of the results of this work with prior data is difficult since in many cases exact experimental parameters (such as focal-spot radius) are unknown for much of the published work. In some publications, the data have been reduced using focal radii scaled to correct for self-

focusing, making direct comparison with these results impossible.[16] In the few cases for which direct comparison can be made, agreement with this work is mixed. For example, Fradin *et al.*[17] measured the breakdown threshold of NaCl for pulse widths of 10.3 and 4.7 nsec and focal-spot radii of 8.8 to 24 μm. They found a breakdown threshold field of $E_B = 2.1$ MV/cm which had little or no dependence on pulse width or spot size, which is in excellent agreement with our results over the same range of focal volume. In a later work, Fradin *et al.*[18] measured E_B for NaCl over the 15-psec to 10.3-nsec range with focal-spot radii of 8.8 to 15.3 μm. They observed a dependence of the breakdown electric field on pulse width consistent with a $t_p^{-1/4}$ dependence and no focal radius dependence. The weak focal-spot radius dependence we observed over the same range of focal radii is consistent with their results. As shown in Table I, we found a much weaker pulse width dependence for comparable focal radii. However, for smaller focal-spot radii, we did observe a $t_p^{-1/4}$ dependence for the breakdown fields.

The NaCl specimen used in this work was 1 of 13 NaCl crystals tested at 1.06 μm with 31-nsec pulses.[1,2] (See Tables II and III.) The breakdown fields among these 13 specimens varied by a factor of 4.6 for a given focal-spot radius and pulse width. Such sample to sample variations indicate that material defects affect the breakdown measurements and thus make direct comparison with other results questionable. Manenkov[3] reported 1.06-μm measurements for what he claimed was intrinsic NaCl. He reported $E_B = 5.4$ Mv/cm for nsec pulse widths and focal-spot radii equal to either 3.25 or 8.49 μm (both focal radii are called out in the paper but it is not specified which corresponds to the breakdown field given). If the E_B corresponds to the smaller radius, then Table I gives a value 2.8 times larger than the breakdown field reported by Manenkov. If the E_B given corresponds to the larger radius then Table I gives a value 0.6 times smaller than the Manenkov value.

Various physical mechanisms and sources of systematic error have been suggested to explain experimentally observed focal-spot size and pulse-width dependences of laser-induced breakdown. Some workers claim that the observed dependence of E_B on focal radius is due to self-focusing,[19–21] and they scale their results in accordance with the technique suggested by Zverev and Pashkov.[19] Zverev and Pashkov[19] predict that a plot of P_B^{-1} (P_B is the power at which breakdown occurs) versus ω_0^{-2} yields a straight line given by

$$\frac{1}{P_B} = \frac{2}{I_B \pi \omega_0^2} + \frac{1}{P_{cr}} , \tag{4}$$

where P_{cr} is the critical power for self-focusing and I_B is the breakdown intensity. The basic assumption of this procedure is that I_B is the intrinsic breakdown intensity and is independent of the focal-spot radius.

It is clearly seen from Fig. 4 that this scaling technique cannot be used for our experiments. Figure 4 is a plot of P_B^{-1} vs ω_0^{-2} for SiO_2 for pulse widths of 44 psec. All of the data for the different pulse widths follow a similar pattern. Our data cannot be fitted to a straight line for any of the specimens examined. Other workers[21] have reported deviations from the straight-line fit for large spot sizes similar to that shown in Fig. 4. These workers[21] disregarded the large spot size data by arguing that, for large focal radii and powers near P_{cr}, the constant shape solution to the nonlinear wave equation (on which the Zverev and Pashkov[19] procedure is based) is no longer valid. However, this argument cannot explain the small focal radii data shown in Fig. 4.

It has been clearly established that, with the possible exception of a small number of specimens tested by Manenkov,[3] the laser-induced breakdown fields are not intrinsic and vary greatly even for specimens of a given material from the same supplier.[1,2,14] This violation of the basic assumption that the damage is intrinsic casts doubt on previously published data where the Zverev and Pashkov[19] scaling was used to interpret breakdown thresholds.

Another test of the role of self-focusing in laser-damage experiments is the apparent pulse-width dependence due to the transient nature of electrostriction.[22] The extent of the electrostrictive contribution to n_2, the nonlinear index of refraction, decreases as the dimensionless quantity X increases. The quantity X is given by[23]

$$X = \omega_0 / v t_p , \tag{5}$$

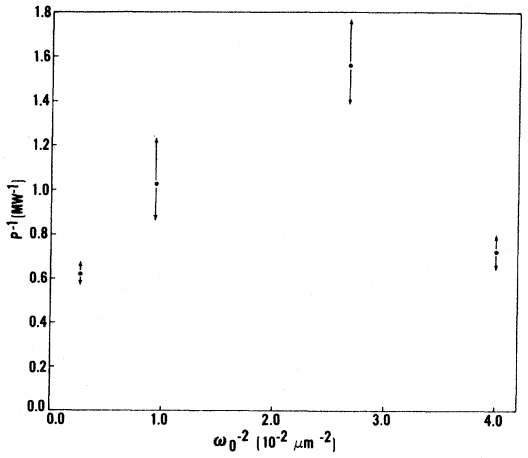

FIG. 4. Representative plot of the inverse of the power, P_B, needed to induce breakdown vs ω_0^{-2}, where ω_0 is the $1/e^2$ radius in intensity at the laser focus calculated using linear Gaussian optics. Here data for SiO_2 using 44-psec (FWHM) pulses are presented.

where v is the speed of sound in the medium. Kerr[23] has shown that for $X < 1$ electrostriction is the dominant self-focusing mechanism and for $X > 1$ the contribution due to electrostriction is inversely proportional to X. Consider the case where the focal spot radius is 19.3 μm. For this case P_B is the largest and the effect of self-focusing should be the greatest. For this focal spot size in NaCl and the longest pulse width (31 nsec) used in this work, X is 0.16 and electrostriction dominates. For the 19.3-μm focal spot radius and a 100-psec pulse width, X is 50, and electrostriction is negligible. Therefore, if self-focusing were significantly contributing to these experimental results, there would be a large pulse-width dependence of E_B for the 19.3-μm focal-spot radius. As can be seen from Table I, the pulse-width-dependent term in the expression for E_B is negligible for a 19.3-μm focal-spot radius for both SiO_2 and NaCl.

A possible explanation of this apparent discrepancy with self-focusing theory is given by including the effects of plasma defocusing.[24] Yablonovitch and Bloembergen[25] showed that the negative n_2 caused by free electrons in a preplasma limits the self-focal radius. Experiments in semiconductors demonstrating these self-defocusing effects are discussed in Refs. 26 and 27. In our experiments the focal radius determined from linear optics is smaller than the limiting self-focal radius calculated using the procedure in Ref. 25. In Ref. 1 it was argued that when these conditions are satisfied the effects of self-focusing can be neglected in calculating focal plane peak intensities. One might ask how self-focusing effects can be compensated by plasma defocusing prior to reaching the breakdown or plasma threshold. For input powers of the order of P_{cr} (the critical power for self-focusing) self-focusing affects the beam diameter significantly only near the geometric focus and the index changes are small. For example, the index change in NaCl for intensities near the breakdown threshold is of the order of 10^{-4}. The index change due to the free-electron plasma is

$$\delta n^- \simeq \omega_p^2/\omega^2 \ , \tag{6}$$

where ω_p is the plasma frequency and ω is the laser frequency.[28] Equation (6) implies that negative index changes on the order of 10^{-4} can be achieved for pre-breakdown plasma densities 10^{-2} times smaller than the critical density required for the plasma frequency to be resonant with the laser. It is therefore possible for plasma defocusing to negate the effects of self-focusing well before damage occurs. A more definitive explanation of the combined role of self-focusing and plasma defocusing will require careful analysis of the nonlinear wave equation including both effects. We have included all the focal parameters used to compute the breakdown fields so that these data can be corrected for self-action effects if future studies show that corrections are needed. Because of the several reasons given above, the data presented in this paper do not include any self-focusing corrections (even though P_B exceeds many estimates of P_{cr}).

Ireland *et al.*[8] pointed out that spherical aberrations due to low f-number focusing optics can give an apparent dependence of breakdown intensity on computed focal-spot radii. Analysis of worst-case aberrations and focal plane scans both confirm that the observed dependence of laser-induced breakdown on focal volume was not due to systematic errors in the determination of focal-spot size.

Bettis *et al.*[29] proposed a model for laser-induced breakdown in solids which incorporated both spot size and pulse-width dependences. Their model, which is based on the dynamics of laser-induced plasma formation, predicts that the bulk breakdown field scales as

$$E_B \propto t_p^{-1/4}\omega_0^{-1} \ . \tag{7}$$

The pulse-width dependence predicted is similar to that observed for small focal volumes in this work but is inconsistent with the observed focal-spot radius dependence and the lack of pulse-width dependence measured for large focal volumes.

Diffusion of energetic electrons out of the region of high electric field is a possible mechanism for the observed focal volume dependence. The model for laser-induced gas breakdown proposed by Kroll and Watson[30] predicts that electron diffusion gives rise to increased breakdown thresholds for small focal volumes. The results of our work for air as shown in Table I and Fig. 3 and prior work[1,31,32] at 1.06, 2.7, 3.8, and 10.6 μm are in reasonable agreement with the predictions of their model if only spot radius dependence is considered. However, diffusion is inconsistent with the observed temporal dependence measured in this work. Diffusion would result in decreased thresholds at short pulse widths since it represents an electron-loss mechanism.

The electron avalanche breakdown model also predicts a pulse-width dependence of laser-induced breakdown.[11] The pulse-width dependence is determined by the ionization rate in the exponential build-up of the free-electron plasma. The observed pulse-width dependence of the breakdown field in NaCl for a 5-μm focal-spot radius is in reasonable agreement with the predictions of the recent theory due to Sparks *et al.*[33] which predicts a $t_p^{-1/4}$ dependence for all focal volumes. Again, agreement is good for small focal volumes, however, the breakdown field for NaCl for the 19.3-μm focal radius is nearly independent of pulse width over the 40- to 31 000-psec region. From the results of Refs. 1 and 2, we know that selected high-purity specimens have breakdown field thresholds at 1.06 μm as high as two to three times greater than the specimen reported in this work. The theory of Sparks *et al.*[33] is for intrinsic

breakdown and does not predict a focal volume dependence and, thus, should not be applied to a defect dominated process.

The focal volume and temporal dependence found in this work is qualitatively consistent with the multiphoton-initiated avalanche breakdown model given in Refs. 1 and 2. That model assumes that for large focal volumes avalanche breakdown is initiated by the conduction-band electrons which are initially present. These starter electrons can be present from thermal ionization of shallow traps, thermionic emission from impurities, etc., therefore the large focal volume damage data will not represent "intrinsic" damage. Table II lists the 1.06-μm, 31-nsec pulsewidth, damage thresholds for various NaCl specimens at several focal-spot radii. These data are for the same specimens used in Refs. 1 and 2. The least-squares fit to Eq. (1) for each specimen is also shown in Table III. Note that the constant term C in Eq. (1) is sample dependent and varies by nearly a factor of 4 for the several NaCl samples shown.

For small focal volumes (focal volumes smaller than the inverse of the zero-field free-electron density) the "starter" electrons for the avalanche must be generated by multiphoton ionization of defect states within the gap. The increased thresholds at small focal volumes are then a direct consequence of having to initiate the avalanche by a higher-order multiphoton process. The rate of increase of the free electron density, N, is then given by

$$\frac{dN}{dt} = \alpha(E,t)N + W_n(E,t)\eta \ , \tag{8}$$

where $\alpha(E,t)$ is the ionization rate for the cascade process, η is the density of defects of ionization energy $\mathcal{E}_D$, and n is the integer part of $\mathcal{E}_D/\mathcal{E}_L$, where $\mathcal{E}_L$ is the laser photon energy. $W_n(E,t)$ is the n-photon ionization rate. The solution to this equation is

$$N(t) = N_0 \exp\left[\int_0^t \alpha(E,t')\,dt'\right] + \int_0^t \eta W_n(E,t') \times \exp\left[-\int_0^{t'} \alpha(E,t'')dt'' \int_0^t \alpha(E,t'')\,dt''\right] dt' \ , \tag{9}$$

where N_0 is the density of free electrons initially present. For large focal volumes the buildup of the free-electron plasma, which leads to breakdown, is dominated by the simple cascade process described by the first term in the above equation and breakdown occurs when $N(t)$ reaches a critical value. For this case the temporal dependence will be determined by the cascade ionization rate $\alpha(E,t)$. For focal volumes smaller than the inverse of the zero-field free-electron density there will be no free electrons within the focal volume, and breakdown is initiated by the second term. The first term of Eq. (8) dominates as soon as starter electrons are available. Braünlich *et al.*[34] have predicted a time dependence for laser-induced damage caused by multiphoton processes. The time dependence is then given by the rate at which the n-photon processes produce starter electrons for the avalanche. However, more information about the n-photon rate is needed in order to determine if this model gives the small focal volume temporal dependence measured in this work.

We have argued that the prebreakdown plasma results in a negative change in the nonlinear index and counters the effects of self-focusing. The model outlined above assumes that for small focal volumes no free electrons are present until they are generated by multiphoton processes. The question of whether or not self-focusing would contribute to the multiphoton processes which initiate breakdown remains unanswered. At what point in time for a psec pulse multiphoton absorption of defects is great enough to cause a carrier density sufficient to negate the effects of self-focusing is now known. However, the effects of self-focusing on the intensity are clearly not in accord with previous theories. The resolution of this question is the subject of our current theoretical and experimental investigations.

V. SUMMARY

The laser-induced breakdown field, E_B, at 1.06 μm, was measured for various focal volumes and laser pulse widths on the same samples. The results of these measurements for solid materials were fitted to a simple linear dependence of E_B on the product $t_p^{-1/4}V^{-1}$, where t_p is the laser pulse width (FWHM) and V is the focal volume. For air the product $t_p^{1/4}E_B$ was linearly dependent on V^{-1}. The essential difference between the results on air and solid materials was that the temporal dependence of E_B for air varies as $t_p^{-1/4}$ for all focal volumes whereas for large focal volumes in the bulk materials the $t_p^{-1/4}$ temporal dependence is masked by the constant term as given in Eq. (1) or Table I. This constant term in Eq. (1) destroys the scaling with $t_p^{-1/4}$ as predicted by avalanche breakdown theory and requires the experimenter to perform damage experiments at several pulse widths, as was done in this work. These results presented here are consistent with a qualitative model for defect dominated laser-induced breakdown which incorporates avalanche breakdown as well as multiphoton ionization of defect levels. Other current models are either inadequate or inconsistent with the results presented here.

ACKNOWLEDGMENTS

The authors acknowledge the support of the Naval Weapons Center, the Office of Naval Research, The Robert A. Welch Foundation, and the North Texas State Faculty Research Fund.

*Some of this work was performed while employed by the Naval Weapons Center, China Lake, Calif. 93555.

[1]M. J. Soileau, Ph.D. thesis (University of Southern California, 1979) (unpublshed).

[2]M. J. Soileau, M. Bass, and P. H. Klein, in *Proceedings of the 11th Annual Symposium on Laser-Induced Damage to Optical Materials* [Natl. Bur. Stand. (U.S.), 1981].

[3]A. A. Manenkov, Natl. Bur. Stand. (U.S) Spec. Publ. 509, 445 (1977).

[4]In Ref. 1, for nsec pulses, it was found that the intensity I_B necessary for breakdown varied as $I_B = K/V + D$, where K and D were constants. This is not inconsistent with the present data since the first term in the square of the empirical equation for the volume dependence of the field is negligible for nsec pulses (i.e., $E_B^2 = K^2/V^2 + 2KD/V + D^2$, where $K^2/V^2 << 2KD/V + B^2$). The difference is observed when the temporal dependence for psec pulses is included.

[5]Quantel model YG-40; 928 Benecia Avenue, Sunnyvale, Calif. 94086.

[6]W. H. Glenn and M. J. Brienza, Appl. Phys. Lett. 10, 221 (1967).

[7]D. J. Bradley and G. H. C. New, Proc. IEEE 62, 313 (1974).

[8]C. L. M. Ireland, A. Yi, J. M. Aaron, and C. Grey Morgan, Appl. Phys. Lett. 24, 175 (1974).

[9]J. P. Anthes and M. Bass, Appl. Phys. Lett. 32, 412 (1977).

[10]*Proceedings of the Annual Conference on Laser Damage,* edited by A. J. Glass and A. H. Guenther (American Society for Testing Materials, Philadelphia, 1969), Spec. Publ. 469; Natl. Bur. Stand. (U.S) Spec. Publ. 341 (1970); 356 (1971); 372 (1972); 387 (1973); 414 (1974); 435 (1975); 462 (1976); 509 (1977); 54 (1978).

[11]Nicolaas Bloembergen, IEEE J. Quantum Electron. QE-10, 375 (1974).

[12]David W. Fradin, Laser Focus 41, 45 (1974).

[13]W. Lee Smith, Opt. Eng. 17, 489 (1978).

[14]D. Olness, Appl. Phys. Lett. 8, 283 (1966).

[15]Y. Yasojima, M. Takeda, and Y. Inuishi, Jpn. J. Appl. Phys. 7, 552 (1968).

[16]W. Lee Smith, J. H. Bechtel, and N. Bloembergen, Opt. Commun. 18, 592 (1976).

[17]D. W. Fradin, E. Yablonovitch, and M. Bass, Appl. Opt. 12, 700 (1973).

[18]D. W. Fradin, N. Bloembergen, and J. P. Letelier, Appl. Phys. Lett. 22, 635 (1973).

[19]G. M. Zverev and V. A. Pashkov, Sov. Phys. JETP 30, 616 (1970).

[20]David W. Fradin, IEEE J. Quantum Electron. QE-9, 954 (1973).

[21]W. Lee Smith, J. H. Bechtel, and N. Bloembergen, Phys. Rev. B 12, 706 (1975).

[22]W. Lee Smith, J. H. Bechtel, and N. Bloembergen, Phys. Rev. B 15, 4039 (1977).

[23]Edwin L. Kerr, Phys. Rev. A 4, 1195 (1971).

[24]R. W. Hellwarth, Natl. Bur. Stand. Spec. Publ. 341, 67 (1970).

[25]E. Yablonovitch and N. Bloembergen, Phys. Rev. Lett. 29, 907 (1972).

[26]A. A. Borshch, M. S. Brodin, and N. N. Krupa, Sov. J. Quantum Electron. 7, 1113 (1977).

[27]Yu. K. Danileiko, A. A. Manenkov, and A. V. Sidorin, Natl. Bur. Stand. Spec. Publ. 541, 305 (1978).

[28]J. Marburger, in *Progress in Quantum Electronics* (Pergamon, New York, 1975), pp. 35–110.

[29]J. R. Bettis, R. A. House II, and A. H. Guenther, Natl. Bur. Stand. Spec. Publ. 462, 338 (1976).

[30]Norman Kroll and Kenneth M. Watson, Phys. Rev. A 5, 1883 (1972).

[31]D. E. Lencioni, Appl. Phys. Lett. 23, 12 (1973).

[32]M. J. Soileau, Appl. Phys. Lett. 35, 309 (1979).

[33]M. Sparks, T. Holstein, R. Warren, D. L. Mills, A. A. Maradudin, L. J. Sham, E. Loh, Jr., and F. King, Natl. Bur. Stand. (in press).

[34]P. Braünlich, A. Schmid, and Paul Kelley, Appl. Phys. Lett. 26, 150 (1975).